

[Original]

## Adhesive Ability of a Dental Adhesive Resin (4-META/MMA-TBB) to As-polished, HNO<sub>3</sub> Treated, and Oxidized Surfaces of the Ni-Cr Alloy

Hiroki OHNO, Yoshima ARAKI, Kazuhiko ENDO, Isao KAWASHIMA,  
Yuro YAMANE, and Masahiro SAGARA

Department of Dental Materials Science, School of Dentistry,  
HIGASHI-NIPPON-GAKUEN UNIVERSITY  
(Chief: Prof. Hiroki OHNO)

### Abstract

The adhesive ability of dental adhesive resin containing 4-META to three different surface states of Ni-Cr alloy which were removed surface irregularities, as-polished, conc. HNO<sub>3</sub> treated, and oxidized surfaces, was studied to evaluate an effect of chemical bonding. A evaluation was performed on the basis of bonding strength obtained from tensile tests and failure types obtained from observation of the fracture. To rapidly evaluate the adhesive ability, the bonded specimens were subjected to thermal stress by thermal cycle using liquid nitrogen. The surface structures were analyzed by reflection electron diffraction.

On the as-polished surface, the adhesive ability of the Ni-Cr alloy is inferior to the Co-Cr alloy. Reflection electron diffraction shows an amorphous structure for the as-polished Co-Cr alloy and an alloy structure of the substrate for the as-polished Ni-Cr alloy. Excellent adhesive ability to the Ni-Cr alloy, which is comparable with that of the Co-Cr alloy, was obtained by treating the as-polished surface by conc. HNO<sub>3</sub> solution and maintained during the severe thermal cycle.

The Ni-Cr alloy oxidized at 300°C for 5 min in air, which is covered with NiO, shows a lower adhesive ability, similar to that of oxidized Co-Cr alloy.

**Key words :** adhesive ability, dental adhesive resin, Ni-Cr alloy, surface pre-treatment

### 1 . Introduction

Many studies have reported improvements in adhesion of dental adhesive resin to the dental alloys by treating the alloy surface. There are several surface pre-treatment methods for Ni-Cr alloys: immersion in conc. HNO<sub>3</sub> solution after etching with HCl<sup>1)</sup>; immersion in

solutions containing an oxidizing agent after sand-blasting<sup>2,3</sup>); etching and passivating by an electrochemical method<sup>4</sup>); and spraying of molten metal on the alloy surface.<sup>5</sup> These methods increase bonding strength by increasing the mechanical retention and chemical affinity between the adhesive resin and alloys. However, it is necessary to separate the contribution of these two effects to evaluate how the alloy surface structure improves the resin adhesion.

To evaluate the chemical effects on the adhesion, we have studied resin adhesion to Co-Cr alloy surfaces which were polished metallographically, and the relationship between bonding strength and surface structure which was analyzed by Electron Spectroscopy for Chemical Analysis(ESCA).<sup>6,7</sup>

The present study reports the adherence of the dental adhesive resin, 4-META/MMA-TBB, to three metallographically polished pretreated surfaces of Ni-Cr alloy, as-polished, conc. HNO<sub>3</sub> treated, and oxidized at high temperature. The alloy surface structures were examined by reflection electron diffraction. The bonded specimens were subjected to thermal stress by the thermal cycle method using liquid nitrogen as reported previously,<sup>6</sup> to rapidly evaluate the adhesive ability. The evaluation of the adhesive ability was made on the basis of the bonding strength measured by a tensile test and observation of fracture appearances in the fracture area. These results for the Ni-Cr alloy were compared with that of Co-Cr alloy previously reported.<sup>6</sup>

## II . Experimental Procedure

### 1. Materials

A 70 mass% Ni-30% Cr alloy was used.

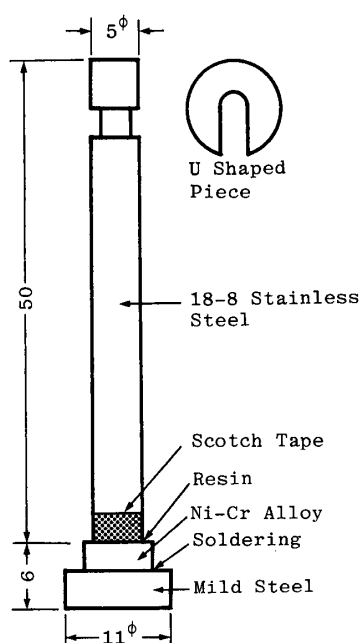


Fig. 1 Tensile test piece of Ni-Cr alloy for bonding strength measurements.

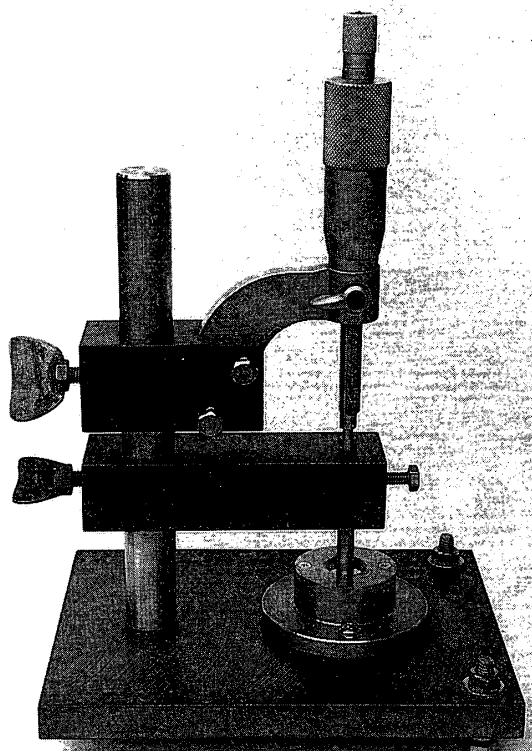


Fig. 2 Adhesion apparatus used to bond the stainless steel rod vertically to the Ni-Cr alloy surface and to maintain a constant 50 μm resin layer thickness.

The alloy was prepared by melting Ni and Cr of a purity better than 99.99% in an alumina Tammann tube under an argon atmosphere using a high frequency induction furnace. The alloy was cut into small chips and the chips were soldered to a mild steel disk as shown in Fig. 1. The dental adhesive resin containing 4-META (4-metacryloxy-ethyl trimellitate anhydride)<sup>8)\*</sup> was used in the present study.

## 2. Pre-treatment of the Alloy Surface

The Ni-Cr alloy specimens were polished metallographically to eliminate any mechanical factors affecting the bonding strength. There were three different surface states: as-polished, conc. HNO<sub>3</sub> treated, or oxidized. The conc. HNO<sub>3</sub> treated surface was obtained by immersing the specimen for 15 min in the conc. HNO<sub>3</sub> solution at room temperature. Both the as-polished and HNO<sub>3</sub> treated specimens were rinsed with distilled water. The oxidized specimen was obtained by heating for 5 min in air at 300°C. After the surface treatments the specimens were stored in desiccator with silica gel before the adhesion experiments.

## 3. Adhesion Experiments

As shown in Fig. 1, the Ni-Cr alloy specimen and 5 mm $\phi$  18-8 stainless steel rod were attached with the adhesive resin for a tensile test to measure the bonding strength. Figure 2 shows the adhesion apparatus with a micrometer which was used for two purposes: to attach the stainless steel rod vertically to the Ni-Cr alloy surface and to maintain a constant 50  $\mu$ m thick resin layer. The effect of the excess resin at the point of adhesion can be eliminated by Scotch Tape on the stainless steel rod as shown in Fig. 1. The bonded specimens were stored at 40°C in a dry chamber for 24 hr before the test.

## 4. Thermal Cycle and Tensile Test

The specimens were subjected to 20 thermal cycles from liquid nitrogen (-195.8°C) to water temperature (40°C), alternately for 1 min each before the tensile test. The test was performed on a testing machine<sup>†</sup> with a load speed of 2 mm/min, after inserting a U shaped piece in the groove of the stainless steel rod (Fig. 1). The fractured area was observed by a profile projector after the test.

## 5. Reflection Electron Diffraction

Reflection high energy electron diffraction patterns were obtained by an electron microscope<sup>‡</sup> with 100 kV accelerating voltage. The camera constant was calibrated with the transmission diffraction pattern of a gold film immediately before and after taking the reflection patterns. The compounds on the alloy surface were identified from Debye-Scherrer powder patterns and the JCPDS card-index on the basis of the measured lattice spacings.

---

\* SUN MEDICAL, Super Bond C & B, Kyoto, Japan

† Shimadzu, Auto-Graph, Kyoto, Japan

‡ Hitachi, H-500, Tokyo, Japan

### III . Results

#### 1. Failure Types and Bonding Strength

Four failure types which are classified in Fig. 3 were observed on the fractured surface: Type I is a failure in the resin (cohesive failure); Type II is a partly cohesive failure and partly interface failure at the Ni-Cr alloy surface; Type III contains a cohesive failure at the central area and an interface failure at the periphery of the Ni-Cr alloy surface; Type IV is a mixture of Types II and III, which is observed when the specimens were subjected to thermal stress.

Figure 4 is the measured bonding strength for the tensile test obtained from the as-polished surface, shown with the notations of the failure types in Fig. 3. The values shown in the left half is the bonding strengths without the thermal cycle (non-thermal cycle) and in the right half with the thermal cycle. The horizontal lines in the figures indicate the average of the repeated values. With the non-thermal cycle, the average bonding strength is 382 kgf/cm<sup>2</sup> and the observed failures are Types I and II, while with the thermal cycle specimens show interface failure at the periphery (types III and IV) with a lower average bonding strength, 322 kgf/cm<sup>2</sup>.

Figure 5 shows the measured bonding strengths and failure types obtained from the specimens with surfaces treated by conc. HNO<sub>3</sub> solution. The bonding strengths with and without the thermal cycle are 402 kgf/cm<sup>2</sup> and 381 kgf/cm<sup>2</sup> and there is no statistically significant difference. Adhesive ability is excellent because the strength does not decrease with the thermal cycle and all the failures are Type I.

Figure 6 shows the results obtained from the specimens oxidized at 300°C. Without the thermal cycle, the result 338 kgf/cm<sup>2</sup>, is lower than as-polished and the failure is Type II in 16 of 20 tests. Further, after the thermal cycle treatment the strength decreased to 247 kgf/cm<sup>2</sup> and failures are of Types III and IV.

#### 2. Analysis of Surface Structure by Reflection Electron Diffraction

Figure 7 shows the reflection electron diffraction pattern obtained from the surface of the as-polished specimen. In Table 1, the observed lattice spacings and intensities of the diffraction rings are shown together with data obtained from the Ni-Cr alloy powder by the Debye-Scherrer method. Except for weak 222 and 400 reflections, the observed lattice spacings and intensities coincide with the X-ray diffraction in the strong intensity reflections, showing that the electron diffraction pattern diffracts from the alloy substrate.

Figure 8 shows the reflection electron diffraction pattern obtained from the specimen oxidized at 300°C. It is impossible to precisely measure the lattice spacings from the very diffuse diffraction pattern which shows an extremely thin oxide layer formed on the alloy surface. The alloy specimen was heated for 5 min at 500°C in air to obtain the sharp diffraction pattern shown in Fig. 9. Both the patterns in Figs. 8 and 9 are considered to be the same diffraction patterns from the coincidence of both the ring sizes and intensities. In Table 2, the observed lattice spacings and intensities of the diffraction rings obtained from

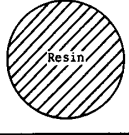



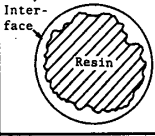



Failure type	Observed figure	Notation
I		
II		
III		
IV		

Fig. 3 Observed failure types and their notations.

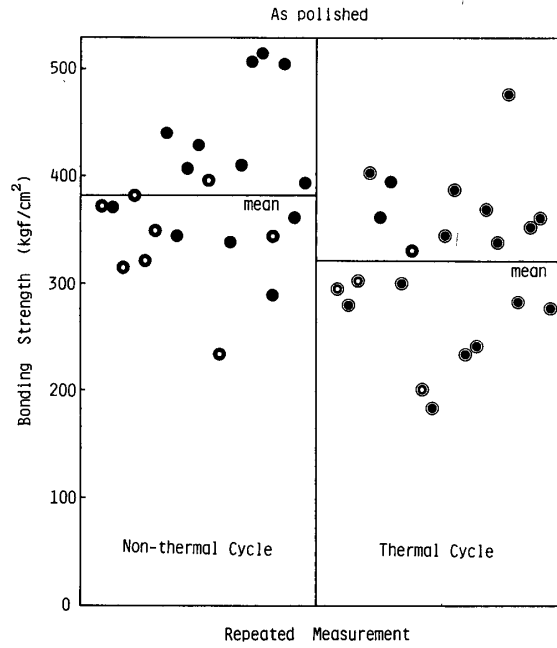


Fig. 4 Results of bonding strength measurements obtained from the specimens bonded to the as-polished Ni-Cr alloy surface. The left half is the bonding strength without thermal cycle (non-thermal cycle) and the right with the thermal cycle. The horizontal line shows the average of the repeated tests.

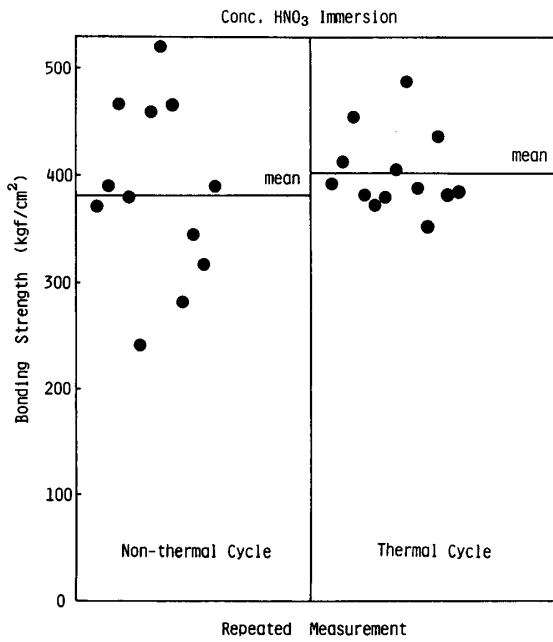


Fig. 5 Results of bonding strength measurements obtained from the specimens treated by HNO<sub>3</sub> solution.

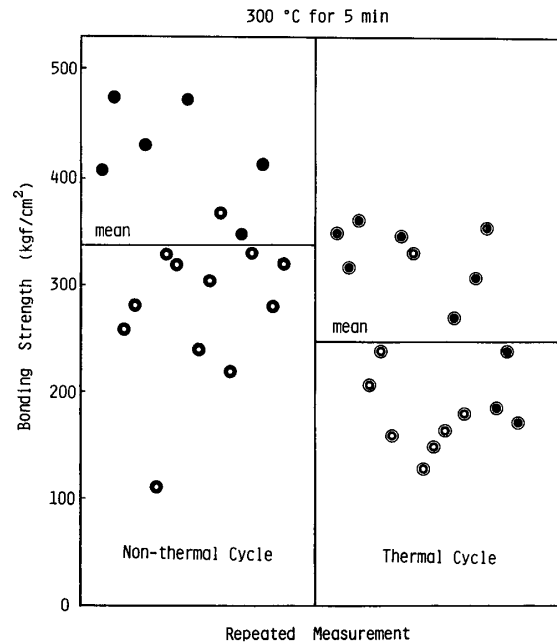


Fig. 6 Results of bonding strength measurements obtained from the specimens oxidized at 300°C.

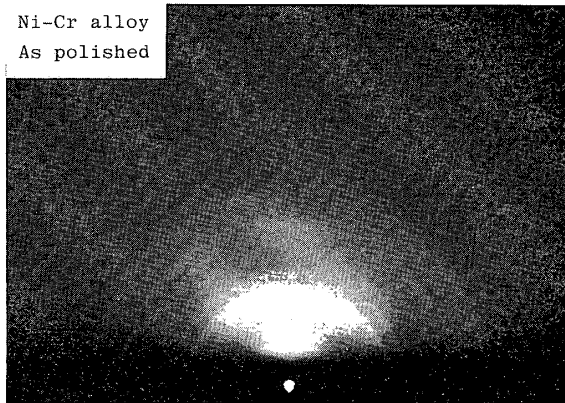


Fig. 7 Reflection electron diffraction pattern obtained from the surface of the as-polished specimen.

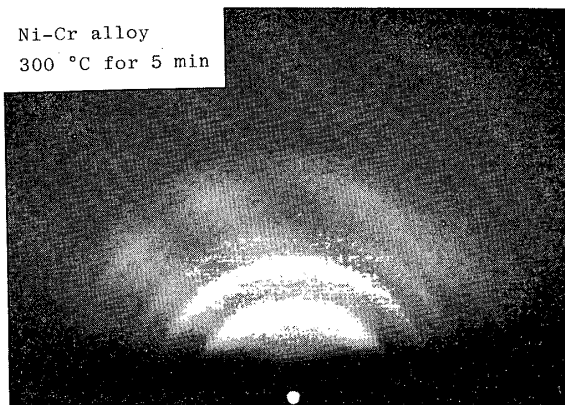


Fig. 8 Reflection electron diffraction pattern obtained from the specimen oxidized at 300°C.



Fig. 9 Reflection electron diffraction pattern obtained from the specimen oxidized at 500°C.

Table 1 Lattice spacings and intensities observed by reflection electron diffraction, obtained from the as-polished specimen (Fig.7), with data obtained from the Ni-Cr alloy powder by Debye-Scherrer method.

Measured values by reflection electron diffraction (As polished)		Measured values by X-ray diffraction*		
		Alloy		
dÅ	I	dÅ	I	hkl
2.10	s	2.063	vs	111
1.80	m	1.782	s	200
1.28	m	1.259	m	220
1.08	m	1.076	m	311
		1.030	vw	222
		0.8929	vw	400
0.834	w	0.8197	w	331
0.813	w	0.7991	w	420

\* Debye-Scherrer method

Table 2 Lattice spacings and intensities observed by reflection electron diffraction, obtained from the oxidized specimen (Fig.9), with data of NiO obtained from JCPDS card.

Measured values by reflection electron diffraction (500 °C for 5min)		Measured values by X-ray diffraction*		
		NiO		
dÅ	I	dÅ	I/I <sub>1</sub>	hkl
2.43	s	2.410	91	111
2.08	vs	2.088	100	200
1.48	vs	1.476	57	220
1.26	m	1.259	16	311
1.21	m	1.206	13	222
1.05	w	1.0441	8	400
0.960	w	0.9582	7	331
0.934	m	0.9338	21	420
0.851	m	0.8527	17	422
0.806	vw	0.8040	7	511

\* JCPDS card

Fig. 9 are shown together with the data for NiO from the JCPDS card-index, showing that the oxidized specimens are covered with NiO.

#### IV. Discussion

##### 1. Thermal Cycle and Failure Type

In a butt joint as in the present study, thermal stress generated in an adhesive is considered to be a function of both the diameter and thickness of the adhesive layer, and the stress is large at the periphery and zero at the center of adhesion.<sup>9)</sup> If chemical bonding between the alloy surface and the adhesive resin is weak, cracks at the resin/alloy interface propagate from the periphery to a point where the thermal stress balances with the adhesive force, producing a Type III failure.

The adhesive ability is usually determined on the basis of the measured bonding strength. However, the measured bonding strengths scatter in the range from 230 kgf/cm<sup>2</sup> to 510 kgf/cm<sup>2</sup> as shown in Fig. 5 (non-thermal cycle) even when all failures are Type I failures. The scatter arises from inhomogeneities in the materials such as air bubble inclusions and variations in the monomer/polymer ratio, and is not caused by chemical factors at the adhesion interface.

In the non-thermal cycle case, the three surface states do not show clearly different bonding strengths, as shown in Figs. 4, 5, and 6. Differences of surface states, however, appears in the failure types because the failure type for both the as-polished and oxidized surfaces is Types I and II and for the conc. HNO<sub>3</sub> treated surface only Type I. Further, the failure types clearly show that the adhesive ability for the conc. HNO<sub>3</sub> treated surface is superior to that for both the as-polished and oxidized surfaces. Observation of the failure types is important to evaluate the adhesive ability, because fracture types rather than the bonding strength sensitively reflect the state of the alloy surface.

As a clinical thermal cycle method, the bonded specimens are subjected to thermal stress induced by repetition of several thousand times between 60°C and 4°C.<sup>10)</sup> However, this thermal cycle method necessarily takes a long time for evaluation of adhesive ability and further induces deterioration in the resin by the water penetrating into the resin during the thermal cycles. By the thermal cycle method used in the present study, it is possible to perform many tests in a short time and to examine only the adhesive ability at the adhesion interface without deterioration of the resin.

##### 2. Comparison between Adhesive Ability to Ni-Cr Alloy and Co-Cr Alloy

###### 1) As-polished Surface

Figure 10 shows the results of the failure types and bonding strength for the as-polished Co-Cr alloy reported previously.<sup>6)</sup> In the non-thermal cycle case, only the Type I failure appears in the Co-Cr alloy and both the Types I and II in the Ni-Cr alloy (Fig. 4). The appearance of Type II shows that the Ni-Cr alloy has a worse alloy surface for the resin adhesion than the Co-Cr alloy. Differences in the alloy surface states is clearly shown by the

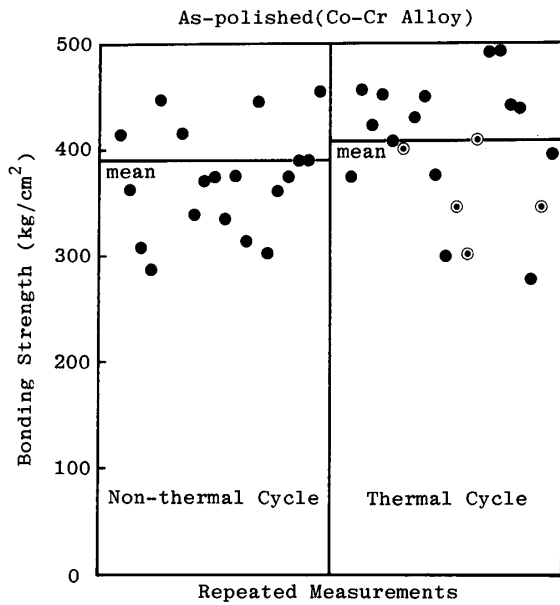


Fig.10 Results of bonding strength measurements obtained from the as-polished Co-Cr alloy specimens.<sup>6)</sup>

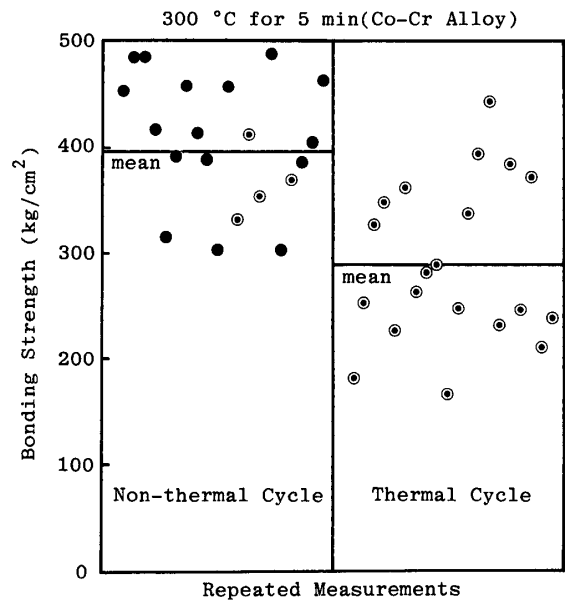


Fig.11 Results of bonding strength measurements obtained from the Co-Cr alloy specimens oxidized at 300°C.<sup>9)</sup>

failure types after the thermal cycle.

There are several reports on adhesion of 4-META resin to Ni-Cr and Co-Cr alloys showing two different results: One reports that Ni-Cr alloys are superior to the Co-Cr alloys<sup>2)</sup> and others report the opposite.<sup>3,8)</sup> The present study which examined only chemical factors and not mechanical factors on the adhesion shows that the Co-Cr alloy is superior to the Ni-Cr alloy.

The reflection electron diffraction pattern obtained from the as-polished Co-Cr alloy surface shows no diffraction rings, indicating that the surface is covered with an amorphous film.<sup>6)</sup> The result coincides with reports<sup>11)</sup> of an amorphous passivated film on the alloy containing Cr. The passive film on the Ni-Cr alloy surface is not sufficiently amorphous as the diffraction pattern shows the substrate to have an alloy structure.

## 2) Oxidized Alloy Surface

Figure 11 shows the results of bonding strength measurements reported previously<sup>6)</sup> for Co-Cr alloy oxidized at 300°C for 5 min. With the thermal cycle, interface failure of the oxidized surface of both alloys occurred at the periphery of the adhesion and the bonding strength decreases. The failure types and bonding strength indicate that the adhesive ability is lowered by oxidizing the Ni-Cr and Co-Cr alloys. The reflection electron diffraction shows that after oxidizing at 300°C, the Ni-Cr alloy is covered with NiO and the Co-Cr alloy with Co<sub>3</sub>O<sub>4</sub>.<sup>6)</sup> Metal oxides adsorb H<sub>2</sub>O in chemisorbed and physisorbed states.<sup>12)</sup> The authors have estimated that deterioration of bonding is due to adsorbed water on the oxide layer<sup>6)</sup> and this has been shown experimentally.<sup>7)</sup> These results indicate that the fine structure on the alloy surface affects the adhesive ability.



### 3. Increase of Adhesive Ability of Ni-Cr Alloy Surface Treated by Conc. HNO<sub>3</sub> Solution

Yamashita<sup>2)</sup> and Tanaka, et al.<sup>3)</sup> have reported that the Ni-Cr alloy surface treated by only sand-blasting has a lower adhesive durability, however, good durability, comparable with that of Co-Cr alloys was obtained by treating the Ni-Cr alloy with either conc. HNO<sub>3</sub> or a solution containing oxidizing agents. In the case of a metallographically polished Ni-Cr alloy surface which removed surface irregularities, treatment by conc. HNO<sub>3</sub> solution protects against the severe conditions of the thermal cycle in the present study, and it also shows excellent adhesive ability as shown in Fig. 5.

To clarify the reason for this both the as-polished and conc. HNO<sub>3</sub> treated surfaces were analyzed by Electron Spectroscopy for Chemical Analysis (ESCA). After treating by conc. HNO<sub>3</sub> solution Cr concentration at the alloy surface was 1.5 times that of the as-polished surface. Further, analysis of the O 1s spectrum revealed that oxygen originating in oxygen bonded Cr, Cr-O-Cr, on the surface treated by conc. HNO<sub>3</sub> was higher than on the as-polished surface, showing the formation of a firm passive film. Details of these results will be reported in the next paper.

### ACKNOWLEDGMENT

This work has been partially supported by a Grant-in-Aid for Scientific Research of the Ministry of Education, Science and Culture of Japan.

### References

1. Tanaka, T., Nagata, K., Takeyama, M., Atsuta, M., Nakabayashi, N., and Masuhara, E.: 4-META opaque resin — A new resin strongly adhesive to nickel-chromium alloy, *J. Dent. Res.*, 60(9); 1697-1706, 1981.
2. Yamashita, A. and Yamami, T.: Procedures for applying adhesive resin (MMA-TBB) to crown and bridge restorations, (Part 1) The influence of dental non-precious alloys and the treatment of inner surface of metal to adhesion, *J. Japan Prosth. Dent.*, 26(3); 130-137, 1982.
3. Tanaka, T., Fujiyama, E., Shimizu, H., and Atsuta, M.: Study on surface treatment of non-precious alloys for adhesion bridge, *ibid.*, 27(4); 54-60, 1983.
4. Yamashita, A., Yamami, T., Ishii, M., Yamaguchi, T., and Uramoto, T.: Procedures for applying adhesive resin (MMA-TBB) to crown and bridge restorations, (Part 3) The Ni-Cr alloys for adhesive resin and its adhesive strength and durability, *ibid.*, 26(6); 22-31, 1982.
5. Shinohara, N., Tojinbara, O., Akita, H., Kakiuchi, T., and Jimi, T.: Studies on the adhesive strength between adhesive resins and each metal surface-treated by wire explosion spray, (Part 2) Adhesive shear strength between Ni-Cr alloy surface-treated by wire explosion spray and adhesive resin (Super Bond C & B), *ibid.*, 28(5); 165-169, 1984.
6. Ohno, H., Araki, Y. and Sagara, M.: The adhesion mechanism of dental adhesive resin to the alloy — Relationship between Co-Cr alloy surface structure analyzed by ESCA and bonding strength of adhesive resin —, *Dent. Mater. J.*, 5(1); 46-65, 1986.
7. Ohno, H., Araki, Y., Sagara, M., and Yamane, Y.: The adhesion mechanism of dental adhesive resin to the alloy — Experimental evidence of the deterioration of bonding ability due to adsorbed water on the oxide layer —, *Dent. Mater. J.*, 5(2); 211-216, 1986.

8. Takeyama, M., Kashibuchi, S., Nakabayashi, N., and Masuhara, E.: Studies on dental self-curing resins, (Part 17) Adhesion of PMMA with bovine enamel or dental alloys, *J. Japan Soc. Dent. Appar. Mat.*, 19(47); 179-185, 1978.
9. Obata, Y. and Inoue, Y.: Analysis of residual stress at adhesion layer, *J. Chemi. Industry*, 61(1); 39-42, 1958.
10. Tanaka, T., Nagata, K., Nakabayashi, N., and Masuhara, E.: Application of 4-META on adhesive opaque resin, (Part 2) Improvement of adhesive stability, *J. Japan Soc. Dent. Appar. Mat.*, 20(52); 221-227, 1979.
11. Rhodin, T.N.: Oxide films on stainless steels, *Corrosion NACE*, 12 : 41~53, 1956.
12. Morimoto, T., Katayama, N., Naono, H., and Nagao, M.: The heat of immersion of ferric oxide in water, *Bull. Chem. Soc. Japan*, 42; 1490-1493, 1969.

## Ni-Cr 合金の表面処理（研磨したまま、濃硝酸処理、高温酸化処理）と接着性レジンの接着性

大野 弘機, 荒木 吉馬, 遠藤 一彦,  
川島 功, 山根 由朗, 相良 昌宏

東日本学園大学歯学部歯科理工学講座

(主任：大野 弘機 教授)

Ni-Cr 合金について、接着性の化学的結合の優劣のみを比較するため、合金表面の凹凸を除き、鏡面状態の3つの合金表面（研磨したまま、濃硝酸処理、高温酸化処理）に対する接着性レジンの接着性を検討した。接着性の評価は接着部の破壊様式と引張試験から求めた接着強さをもとに行った。短時間に接着性を評価するために、接着試料に液体チッ素を用いた熱サイクルを施した。表面状態は反射電子回折で同定した。

研磨したままでは、Ni-Cr 合金は Co-Cr 合金よりも接着性が劣る。反射電子回折によると、Co-Cr 合金表面は非晶質構造であるが、Ni-Cr 合金の場合、下地の合金からの回折線が得られた。Ni-Cr 合金の接着性が劣るのは十分な不動態被膜が形成されていないためと考えられた。しかし、Ni-Cr 合金を濃硝酸で処理すると、過酷な熱サイクル後も Co-Cr 合金に匹敵する接着性が得られた。300°Cで 5 min の高温酸化処理を施すと Ni-Cr 合金は薄い NiO の被膜で被われ、Co-Cr 合金と同様に研磨したままよりも接着力が低下した。